Oxidation Reduction Behavior of Iron-Bearing Olivines $(Fe_xMg_{1-x})_2SiO_4$ Used as Catalysts for Biomass Gasification

D. Świerczyński,† C. Courson,† L. Bedel,† A. Kiennemann,*,† and S. Vilminot‡

Laboratoire des Matériaux, Surfaces et Procédés pour la Catalyse, ECPM, UMR 7515-25 rue Becquerel, 67087 Strasbourg Cedex 2, France, and Groupe des Matériaux Inorganiques, IPCMS, UMR 7504-23 rue du Loess, 67037 Strasbourg Cedex, France

Received July 1, 2005. Revised Manuscript Received September 22, 2005

Natural iron-bearing olivines $(Fe_xMg_{1-x})_2SiO_4$ have been recognized as one of the most promising tar-cracking catalytic materials for fluidized bed biomass gasification to produce syngas (H_2 + CO). Iron present in the olivine significantly influences its catalytic activity. However, the Fe^0-active phase cannot be obtained by the reduction of olivine under the catalyst working conditions. A better understanding of olivine's behavior in oxidizing−reducing conditions is crucial for control of its catalytic properties. In this paper, we have demonstrated how the oxidation of iron-bearing olivines leads to the formation of reducible iron oxides dispersed in the iron-depleted olivine matrix. The choice of oxidation−reduction conditions permits us to control the amount of iron extracted from the olivine structure. The mechanism of the oxidation−reduction behavior of a natural olivine has been studied by ^{57}Fe Mössbauer spectroscopy, X-ray diffraction (XRD), scanning electron microscopy (SEM), and temperature-programmed reduction (TPR).

Introduction

Olivine is the most abundant mineral in the Earth's upper mantle,[1] occurring predominantly in igneous rocks. It is an orthosilicate with a general formula of $(Fe_xMg_{1-x})_2SiO_4$ representing a complete solid solution between forsterite, Mg_2SiO_4, and fayalite, Fe_2SiO_4. Because of the high melting point (1890 °C for forsterite and 1205 °C for fayalite), the olivines rich in Mg are used as refractory materials in the ceramic and metallurgical industries. Natural olivine has also been recognized as one of the most promising solid materials for use in fluidized bed biomass steam gasification.[2,3] A pilot plant of biomass steam gasification in a fast internally circulating fluidized bed (FICFB) reactor has recently been operated in Guessing, Austria, using natural olivine. Its presence enhances gas production and quality (40% H_2, 25% CO, 20% CO_2, 10% CH_4) and also drastically decreases tar formation during the process (less than 1 g Nm^{-3}).[4] In fact, olivine has been considered as being a promising tar-cracking material for fluidized bed use,[4−7] presenting a wide range of advantages: thermal stability, activity, abrasion resistance, and a low price. In catalysis, olivine can also be used as a support, particularly for a Ni catalyst[8] used in methane[9] and tar reforming,[10] which could also perform in steam fluidized bed biomass gasification, as it shows both a high activity level and attrition resistance.[11]

The catalytic activity of olivines was proposed to be due to the presence of iron species.[4,12,13] The importance of the iron species presence was also demonstrated by Orio et al.[14] in dolomites, which are similar "tar-cracking" materials. It is then crucial to explore and understand the role of iron in the olivine structure. The gaseous atmosphere in a circulating fluidized bed (FICFB) reactor is alternatively oxidizing and reducing. It is then important to characterize the olivine in these two conditions with respect to the evolution of the iron oxidation state. A hypothesis could be made that metallic iron is important for the olivine's activity. This hypothesis is based on the fact that the same precalcined olivine (with part of the Fe outside of the olivine structure being an iron

* To whom correspondence should be addressed. Tel.: 33-390-2427-66. Fax: 33-390-2427-68. E-mail: kiennemann@chimie.u-strasbg.fr.
† ECPM.
‡ IPCMS.

(1) Ringwood, A. E. In *Composition and Petrology of the Earth's Mantle*; McGraw-Hill: New York, 1975; p 618.
(2) Rapagná, S.; Jand, N.; Kiennemann, A.; Foscolo, P. U. *Biomass Bioenergy* **2000**, *19*, 187.
(3) Hofbauer, H.; et al. 12th European Conference and Technology Exhibition on Biomass for Energy, Industry and Climate Protection; Amsterdam, June 2002.
(4) Rauch, R.; Bosch, K.; Hofbauer, H.; Świerczyński, D.; Courson, C.; Kiennemann, A. Comparison of Different Olivines for Biomass Steam Gasification. Science in Thermal and Chemical Biomass Conversion Conference, Victoria, BC, Aug 30−Sept 20, 2004.
(5) Dayton, D. *A Review of the Literature on Catalytic Biomass Tar Destruction*; Report NREL/TP-510-32815; NREL: Golden, CO, 2002.
(6) Devi, L.; Ptasinski, K. J.; Janssen, F. J. J. G. Olivine as a Tar Removal Catalyst for Biomass Gasifiers. In *Proceedings of the 2nd World Conference & Technological Exhibition on Biomass for Energy, Industry and Climate Protection*, Rome, May 10−14, 2004.
(7) Corella, J.; Toledo, J. M.; Padilla, R. *Energy Fuels* **2004**, *18*, 713.
(8) Świerczyński, D.; Courson, C.; Guille, J.; Kiennemann, A. *J. Phys. IV* **2004**, *118*, 385.
(9) Courson, C.; Udron, L.; Świerczyński, D.; Petit, C.; Kiennemann, A. *Catal. Today* **2002**, *76*, 75.
(10) Świerczyński, D.; Courson, C.; Petit, C.; Kiennemann, A. 1st European Hydrogen Energy Conference, Grenoble, France, Sept 2−5, 2003.
(11) Pfeifer, C.; Rauch, R.; Hofbauer, H.; Świerczyński, D.; Courson, C.; Kiennemann, A. Hydrogen-Rich Gas Production with a Ni-Catalyst in a Dual Fluidized Bed Biomass Gasifier. Science in Thermal and Chemical Biomass Conversion Conference, Victoria, BC, Aug 30−Sept 20, 2004.
(12) Devi, L.; Ptasinski, K. J.; Janssen, F. J. J. G. *Fuel Process. Technol.* **2004**, *86*, 707.
(13) Devi, L.; Craje, M.; Thüne, P.; Ptasinski, K. J.; Janssen, F. J. J. G. *Appl. Catal., A* **2005**, *294*, 68.
(14) Orío, A.; Corella, J.; Narváez, I. *Ind. Eng. Chem. Res.* **1997**, *36*, 3800.

10.1021/cm051433+ CCC: $33.50
Published on Web 01/18/2006

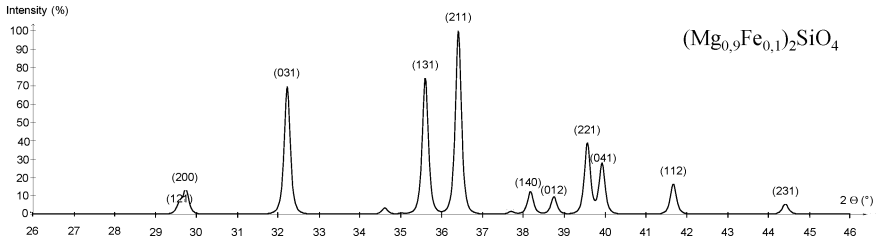

Figure 1. Theoretical diffractogram of $(Mg_{0.9}Fe_{0.1})_2SiO_4$ ($\lambda = 1.5406$ Å).

Table 1. Chemical Composition of Initial Olivine

	Mg	Si	Fe	Ni	Ca	Al	Cr
wt %	30.5	19.6	7.1	0.19	0.20	0.07	0.08

oxide−olivine system), which is performing very well in steam gasification under reducing conditions, as demonstrated by Rapagná[2] and Rauch,[4] does not perform well in gasification with air, as shown by Corella et al.[7] It can be concluded that to activate the olivine, reducing conditions (a high H_2 content in the product gas) are needed to obtain metallic iron.

The thermal transformation of iron-bearing materials in an oxidizing atmosphere represents a large group of solid-state reactions associated with the formation of different iron(III) oxides, which under reducing conditions may result in the formation of iron(II) or metallic iron. The purpose of this work is to bring information about the mechanism of the thermal transformation of Fe^{2+} from olivine under oxidizing and reducing conditions to give a basis for a better understanding of the catalytic performance of olivine in biomass gasification, as well as further improving the transformation by extracting more iron from the olivine structure or by incorporating a more catalytically active metal such as nickel.

Experimental Section

Properties of the Natural Olivine Used. Natural olivine came from an Austrian mine (Magnolithe GmbH). The material was delivered after calcination in air at 1600 °C for 4 h, with crushing and sieving to obtain particle sizes between 400 and 600 μm. This initial calcination is used to improve the olivine's mechanical properties for fluidized bed use. It will later be called the initial olivine (which was tested in the steam gasification of biomass as olivine A elsewhere[4]). Its composition (Table 1), obtained by atomic absorption (CNRS Centre in Vernaison), leads to a mean global formula $(Mg_{0.9}Fe_{0.1})_2SiO_4$ (without taking into account the minority elements Ni, Ca, Al, and Cr).

The specific surface area of this olivine is very low (<1 m^2/g) because of its initial sintering (melting point approximately 1760 °C), and this olivine is considered to be nonporous.

Characterization Methods. The crystalline phases contained in the samples and the structural modifications occurring after calcination and reduction were examined by powder X-ray diffraction (XRD) on a Siemens D500TT diffractometer using Cu Kα radiation ($\lambda = 1.5406$ Å) with a step size of 0.02° 2θ and a step time of 20 s.

Scanning electron microscopy (SEM) was performed on a JEOL 6700 F microscope. The samples were prepared first for observing the surface morphology and for measuring the compositional profiles in the bulk on cut grains. For this purpose, the samples were mounted in epoxy, cut to obtain planar sections, polished, and examined by SEM and X-ray microanalysis.

To quantify the amount of reducible iron, we followed the reducibility of the olivines by performing temperature-programmed reduction (TPR) on 200 mg of catalyst placed in a U-shaped quartz tube (6.6 mm ID). The reductive gas mixture ($H_2 = 0.12$ L h^{-1} and Ar $= 3$ L h^{-1}) passed through a reactor that was heated from room temperature to 950 °C with a slope of 15 °C min^{-1} and then maintained at 950 °C until the end of H_2 consumption (shown by the baseline return). A thermal conductivity detector (TCD) was used for quantitative determination of hydrogen consumption.

The ^{57}Fe Mössbauer spectra were recorded at 77 K using a spectrometer with a triangular waveform with a ^{57}Co source (50 mCi) dispersed in a rhodium matrix. From the obtained spectra, we determined the isomeric shifts in comparison with a metallic iron standard at room temperature. To identify the different forms of iron present in the sample, we fit the spectra with the MossFit computer program.

Results and Discussion

Influence of the Calcination Temperature on the Oxidation of Natural Olivine. *X-ray Diffraction.* Figure 1 shows the theoretical diffractogram of a pure $(Mg_{0.9}Fe_{0.1})_2SiO_4$ phase, modeled with the help of the CaRIne Crystallography[15] program for $\lambda = 1.5406$ Å on the basis of the crystallographic positions of ions in $(Mg_{0.9}Fe_{0.1})_2SiO_4$ given by Nover and Will.[16]

XRD of the initial olivine (Figure 2) shows the same main lines as those in the theoretical diffractogram of $(Mg_{0.9}Fe_{0.1})_2SiO_4$, which are close to those of the Mg_2SiO_4 forsterite.[17] Additionally, the secondary crystalline phases observed are the $MgSiO_3$ enstatite phase,[18] visualized by its 100-intensity line at 28.2° 2θ, and a spinel cubic phase, which could be either γ-Fe_2O_3, Fe_3O_4, or $MgFe_2O_4$ magnesioferrite (and/or members of solid solutions such as $MgFe_2O_4-Fe_3O_4$ and $MgFe_2O_4-\gamma$-Fe_2O_3).[19] XRD does not permit us to distinguish between those three phases, which have nearly the same diffraction patterns.[20] As the initial olivine was previously calcined at 1600 °C for 4 h, the presence of γ-Fe_2O_3 would be surprising; this phase is only a metastable, and the phase transition to hematite occurs at temperatures above 300 °C.[21] Moreover, most authors report the formation of magnetite,[22]

(15) Boudias, C.; Monceau, D. *CaRIne Crystallography 3.1*; Divergent SA: Compiègne, France, 1998.
(16) Nover, G.; Will, G. *Z. Kristallogr.* **1981**, *155*, 27.
(17) Powder Diffraction File 34-0189 (Mg_2SiO_4); International Center for Diffraction Data: Newtown Square, PA.
(18) Powder Diffraction File 19-0606 ($MgSiO_3$); International Center for Diffraction Data: Newtown Square, PA.
(19) Meyer, M.; Rüffler, R. *Hyperfine Interact.* **2002**, *141/142*, 351.
(20) Joint Committee on Powder Diffraction Standards files: Fe_3O_4 (19-269), γ-Fe_2O_3 (39-1346), and $MgFe_2O_4$ (17-464).
(21) Cornell, R. M.; Schwertmann, U. *The Iron Oxides*; VCH: Weinheim, Germany, 1996.
(22) Champness, P. E. *Mineral. Mag.* **1970**, *37*, 790.

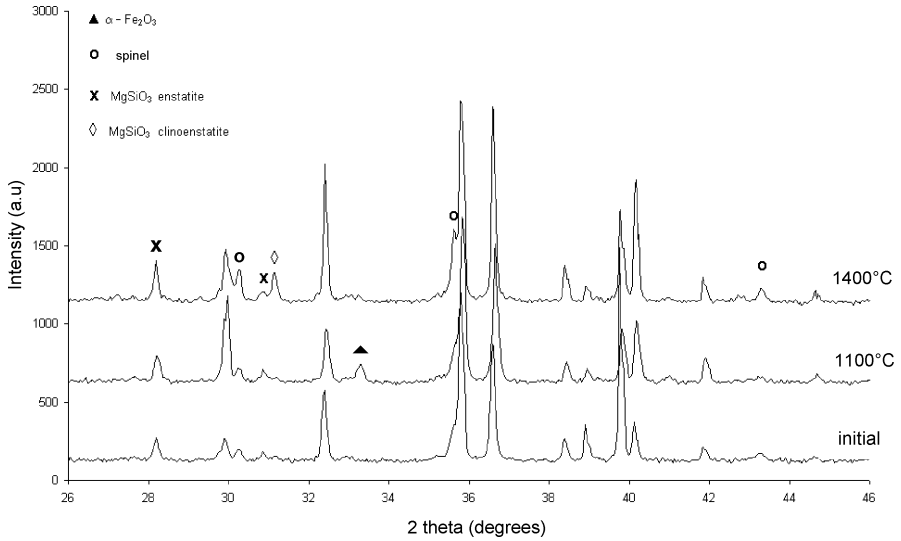

Figure 2. Diffractograms of initial olivine and olivine calcined at 1100 and 1400 °C ($\lambda = 1.5406$ Å).

Table 2. Lattice Parameters and Cell Volumes Obtained by Rietveld Refinements of Olivine Calcined at Different Temperatures.[a]

	Mg_2SiO_4[17]	Fe_2SiO_4[26]	initial olivine	olivine calcined at 400 °C	olivine calcined at 1100 °C	olivine calcined at 1200 °C	olivine calcined at 1400 °C
a (Å)	5.9817(5)	6.0902(5)	5.9870(2)	5.9848(1)	5.9818(2)	5.9838(2)	5.9844(2)
b (Å)	10.1978(8)	10.4805(8)	10.2125(5)	10.2164(3)	10.2028(4)	10.2011(4)	10.2069(4)
c (Å)	4.7553(3)	4.8215(5)	4.7577(2)	4.7582(1)	4.7536(2)	4.7548(2)	4.7560(2)
V (Å^3)	290.07(6)	307.75(8)	290.90(4)	290.93(2)	290.12(4)	290.24(3)	290.51(3)

[a] Literature data for forsterite and fayalite are given for comparison.

Fe_3O_4, or magnesioferrite $MgFe_2O_4$[19,23,24] as being the high-temperature oxidation products of iron-bearing olivine. The presence of the minority phases is then due to the 1600 °C pretreatment giving rise to olivine oxidation.

This initial olivine has been calcined in air in the temperature range between 400 and 1400 °C. The main olivine phase is still observed for all the calcination temperatures (Figure 2), but significant modifications of some line intensities are observed, i.e., lines (200) and (211).

The sample calcined at 400 °C does not show any modification in comparison to the initial olivine. We also notice that the intensity of the main reflection of $MgSiO_3$ is not modified for the initial olivine calcined between 400 and 1100 °C. After calcination at 1100 °C and in addition to the reflections of olivine, we can observe the apparition of the main reflection of α-Fe_2O_3 ($2\theta = 33.2°$) and a slight increase in the intensity of the spinel phase ($2\theta = 30.3$, 35.6, and 43.3°). The presence of iron oxides can be explained by the rejection of iron from the olivine structure caused by the oxidation of iron(II) to iron(III) accompanied by the formation of amorphous silica (not detected by XRD), as indicated by P. E. Champness.[22] Assuming that all iron is rejected, the following reaction can be proposed

$$(Mg_xFe_{1-x})_2SiO_4 + (1-x)O_2 \rightarrow x Mg_2SiO_4 + (1-x)Fe_2O_3 + (1-x)SiO_2 \quad (1)$$

For the sample calcined at 1400 °C, the main line of α-Fe_2O_3 practically dissappears and an increase in the intensity of the main diffraction lines of the spinel phase can be observed. We also notice an increase in the intensity of the main diffraction line of enstatite ($MgSiO_3$). As has been shown for temperatures higher than 1100 °C, silica reacts with olivine to form a pyroxene phase, such as enstatite or protoenstatite (eq 2).[25]

$$SiO_2 + Mg_2SiO_4 \rightarrow 2MgSiO_3 \quad (2)$$

It should be noted that for the sample calcined at 1400 °C, protoenstatite changes into clinoenstatite ($2\theta = 31.1°$).

The variation in the intensities of some olivine lines mentioned previously is then related to the Fe departure. Effectively, if the Mg_2SiO_4[17] and Fe_2SiO_4[26] XRD data are compared, we clearly observe an evolution of the line intensities. In our case, the formation of Mg_2SiO_4 can therefore explain the observed evolution.

Lattice Parameters. For the solid solution of $(Mg_{1-x}Fe_x)_2SiO_4$, the lattice parameters and unit cell volume (V_{cell}) show a linearly increasing dependence on *x* (the ionic radii for 6-fold coordination are 0.65 Å for Mg^{2+} and 0.77 Å for Fe^{2+}).[27] The empiric relation, in accordance with Végard's law, was determined by Schwab and Küstner.[28] The cell parameters of the initial olivine and the olivine calcined at different temperatures (Table 2) were calculated with the Fullprof[29] program after indexation of the diffractograms in the orthorhombic system, space group *Pnmb*, according to

(23) Khisina, N. R.; Khramov, D. A.; Kolosov, M. V.; Kleschev, A. A.; Taylor, L. A. *Phys. Chem. Miner.* **1995**, *22* (4), 241.
(24) Barcova, K.; Mashlan, M.; Zboril, R.; Martinec, P. *J. Radioanal. Nucl. Chem.* **2003**, *255* (3), 529.
(25) Massouch, S.; Perez, A.; Serughetti, J. *Nucl. Instrum. Methods Phys. Res., Sect. B* **1988**, *32*, 71.
(26) Powder Diffraction File 34-0178 (Fe_2SiO_4); International Center for Diffraction Data: Newtown Square, PA.
(27) Wells, A. F. *Structural Inorganic Chemistry*; Oxford University Press: Oxford, U.K., 1962; p 483.
(28) Schwab, R. G.; Küstner, D. *Neues Jahrb. Mineral., Monatsh.* **1977**, *5*, 205.

Table 3. Unit Cell Volume, *x*, and Wt % Iron Present as Iron Oxides in Natural Olivine Calcined at Different Temperatures

T_{calc} (°C) of olivine	V (Å^3)	x (in $(Mg_{1-x}Fe_x)_2SiO_4$)	wt % free Fe (in form of oxides)	wt % free Fe/total Fe
initial	290.90(4)	0.047	3.8	52
400	290.93(2)	0.049	3.6	51
1100	290.12(3)	0.003	6.9	97
1200	290.24(3)	0.010	6.4	90
1400	290.51(3)	0.025	5.3	75

the JCPDS forsterite file.[17] The cell parameters of forsterite and fayalite are given as a reference.

The initial olivine and olivine calcined at 400 °C have practically the same cell-volume parameters. The increase in the calcination temperature from 400 to 1100 °C leads to a contraction of the unit cell after the departure of iron from the olivine structure. On the other hand, the increase in the calcination temperature from 1100 to 1400 °C leads to a small increase in the cell volume, indicating that the quantity of iron that has left the structure after calcination at 1400 °C is slightly lower than that for the calcination at 1100 °C. This phenomenon can be explained on the basis of the thermodynamic stability of olivines and will be discussed later.

If we consider that the solid solution of $(Mg_{1-x}Fe_x)_2SiO_4$ obeys Végard's law, it is possible to deduce the approximate composition of olivine (x) calcined at different temperatures from its cell volume (Table 3). The difference between this composition and the nominal composition ($x = 0.1$) gives the quantity of iron in the form of oxides (free iron).

The maximal quantity of free iron (~7 wt %) can be obtained after calcination at 1100 °C. For higher calcination temperatures, the decrease in the proportion of free iron can be related to the thermodynamic stability discussed later.

Scanning Electron Microscopy. As shown by several authors, the nucleation of precipitates in olivines that are subjected to a high-temperature oxidizing atmosphere occurs heterogeneously on dislocations, which are present because of prior deformation.[30] Iron oxide precipitates occur as rodlike interwoven fingers. SEM performed with backscattered electrons on cut grains for olivine calcined at various temperatures confirms these observations, with the presence of iron-rich areas in the whole depth of the grains. In fact, the bright spots can be attributed to iron-rich phases (olivine calcined at 900 °C, Figure 3). Their number increases in samples previously calcined at 1100 °C, in agreement with the previous XRD results.

Figure 4 shows the changes in morphology of the olivine surface after calcination at different temperatures.

The initial olivine sample presents a smooth surface covered with particles, most likely the products of the oxidation of the iron and secondary phases. Calcination at 1100 °C leads to the appearance of more particles on the surface. After calcination at 1400 °C, a very smooth olivine surface is observed with deposited spinel particles, according to its octahedral shape.

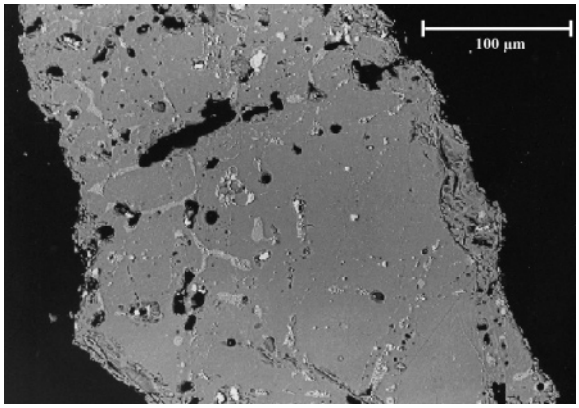

Figure 3. SEM micrograph (backscattered electrons) on cut grain of olivine calcined at 900 °C.

Studies by XRD and SEM permitted us to demonstrate the presence of iron oxides in olivine and their evolution with calcination temperature. We need, however, the information about the quantity of iron with a given degree of oxidation, which will provide a basis for further reducibility studies. To quantify the amount of iron in the different phases, we carried out a study with ^{57}Fe Mössbauer spectroscopy.

Mössbauer Spectroscopy. Figure 5 presents Mössbauer spectra of initial olivine and olivine calcined at 1100 and 1400 °C recorded at the liquid nitrogen temperature (77 K). Let us first analyze the spectrum of the initial olivine.

Three components were identified: one doublet and two sextets. The three theoretical spectra and the result of the sum of the theoretical spectra superimposed on the experimental points are presented in Figure 5. Table 4 sums up the different parameters of subspectra for the olivine calcined at different temperatures.

Table 4 shows that all samples, regardless of the temperature of calcination, contain the Fe^{2+} doublet and two Fe^{3+} sextets.

The quadrupole doublet present in the Mössbauer spectra with an isomer shift of ~1.12 mm s^{-1} and quadrupole splitting of ~3.06 mm s^{-1} is due to Fe^{2+} ions in the olivine structure. This apparent ferrous doublet is in fact a superposition of two doublets caused by Fe^{2+} at the M1 and M2 sites of the olivine lattice. These doublets strongly overlap and are therefore not resolvable; they had to be fitted by one hyperfine pattern.[19]

The two other components are magnetic sextets. The isomer shift values of 0.26 and 0.36 mm s^{-1} are characteristic of Fe^{3+} ions.[31,32]

We have observed by XRD the presence of a spinel phase that could be either γ-Fe_2O_3, Fe_3O_4, $MgFe_2O_4$, or a solid solution between those phases. The presence of γ-Fe_2O_3 was eliminated because of its thermal instability. As for Fe_3O_4, its Mössbauer spectrum at ambient temperature includes two sextets with an isomer shift of $\delta \approx 0.27$ and 0.67 mm s^{-1}

(29) Rodriguez-Carvajal, J. *FULLPROF: Rietveld, Profile Matching and Integrated Intensity Refinement of X-ray Data,* version 3.5d; Leon-Brillouin Laboratory: CEA-Saclay, France, 1998.
(30) Kohlstedt, D. L.; Vander Sande, J. B. *Contrib. Mineral. Petrol.* **1975**, *53*, 13.
(31) Imelik, B.; Védrine, J. C. *Les Techniques Physiques d'Étude des Catalyseurs*; Editions Technip: Paris, 1998.
(32) Greenwood, N. N.; Gibb, T. C. *Mössbauer Spectroscopy;* Chapman & Hall: London, 1971.

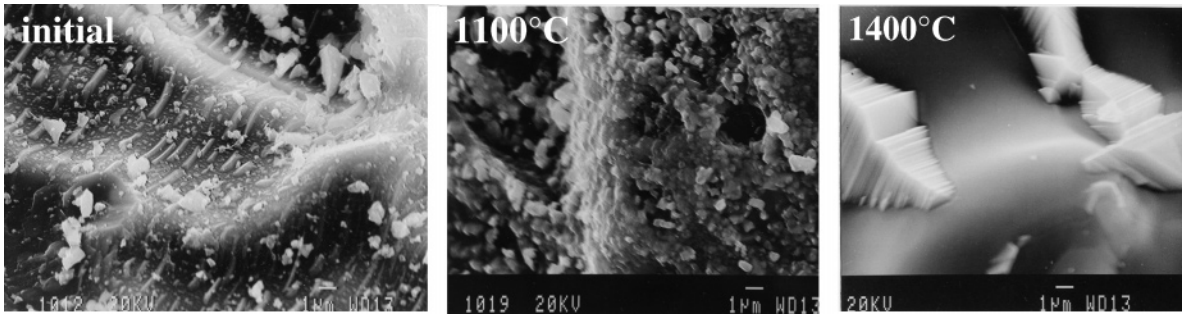

Figure 4. SEM micrograph of olivine calcined at different temperatures.

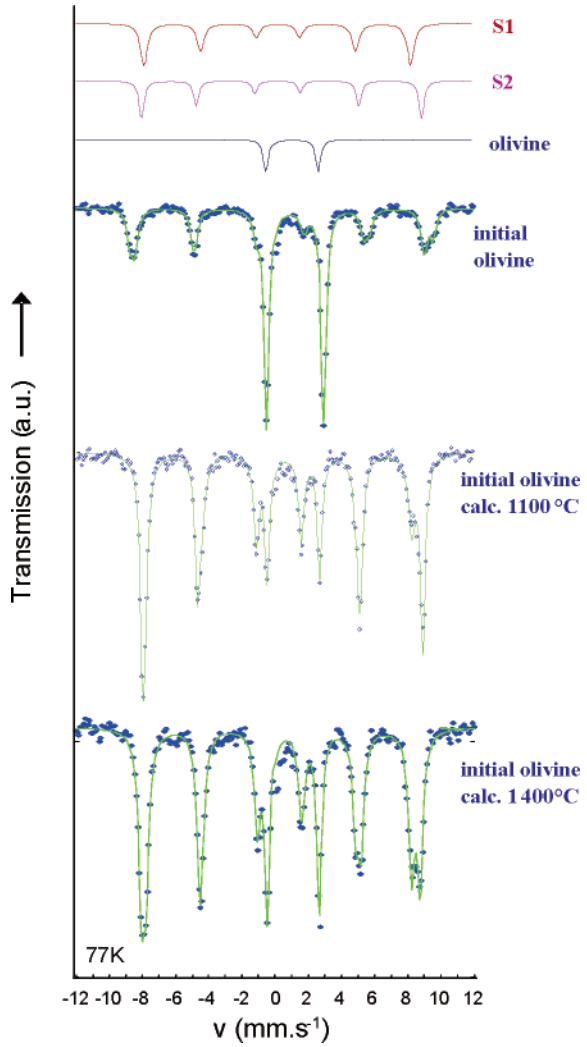

Figure 5. ^{57}Fe Mössbauer spectra at 77 K of initial olivine and olivine calcined at different temperatures; subspectra of the three components are indicated at the top.

and different hyperfine fields of ~490 and ~460 kG.[33] As no sextet with $\delta \approx 0.67$ mm s^{-1} and $H \approx 460$ kG (Fe^{2+}) has been observed, we can eliminate the presence of Fe_3O_4.

The parameters of the first sextet (S1) ($\delta = 0.26$ mm s^{-1}, $\Delta = 0$ mm s^{-1}, and $H = 495$ kG) could be attributed to either γ-Fe_2O_3,[34] previously rejected, or Fe^{3+} in tetrahedral sites of magnesioferrite.[35] This phase is generally described by the formula $(Mg_{1-\lambda}Fe_\lambda)[Mg_\lambda Fe_{2-\lambda}]O_4$, where the parentheses and square brackets denote cation sites of tetrahedral (A) and octahedral [B] coordination, respectively,[36] and λ represents the so-called degree of inversion (defined as the fraction of either the (A) sites occupied by Fe^{3+} cations or the [B] sites occupied by Mg^{2+} cations).

Table 4. Mossbauer Parameters of Components Present in Olivine Calcined at Different Temperatures[a]

	initial olivine	olivine calcined at 1100 °	olivine calcined at 1400 °C
	Doublet Fe^{2+} (olivine)		
δ (m s^{-1})	1.12	1.11	1.12
Δ (mm s^{-1})	3.06	3.06	3.05
H (kG)	0	0	0
R (%)	55	17	20
	Sextet 1 Fe^{3+}		
δ (mm s^{-1})	0.26	0.25	0.25
Δ (mm s^{-1})	0.00	−0.02	0.00
H (kG)	495	497	495
R (%)	31	29	41
	Sextet 2 Fe^{3+}		
δ (mm s^{-1})	0.36	0.36	0.35
Δ (mm s^{-1})	0.00	0.19	0.03
H (kG)	518	523	519
R (%)	14	54	39

[a] δ, isomer shift related to metallic iron; Δ, quadrupole splitting; H, hyperfine field; R, relative area.

The parameters of the second sextet (S2) ($\delta = 0.36$ mm s^{-1}, $\Delta = 0$ mm s^{-1}, and $H = 518$ kG) are characteristic of α-Fe_2O_3[37] or Fe^{3+} ions in octahedral sites of magnesioferrite spinel.[35] No hematite was detected by XRD, probably because of the small particle size or the fact that the amount of the oxide present was too small to be detected by X-ray diffraction (14% total iron present in the hematite phase corresponds to ~1.3 wt % oxide).

The most probable conclusion is that the two sextets are due to a contribution of hematite and magnesioferrite. It is, however, difficult to fit the spectra without additional information. In the following discussion, which concerns the effect of the calcination temperature, different Fe^{3+}-containing phases will not be differentiated.

Mössbauer spectroscopy confirms the rejection of iron after calcination at 1100 and 1400 °C because of its oxidation. At ambient temperature, 55% of the iron is present in the olivine structure and 45% in the form of oxides. After calcination at 1100 °C, only 17% of the iron is present in

(33) *Mössbauer Mineral Handbook*; Stevens, J. G., et al., Eds.; Mössbauer Effect Data Center: Asheville, NC, 1998.
(34) Malysheva, T.; Kurash, V. V.; Yermakov, A. N. *Geokhimiya* **1969**, *11*, 1405.
(35) O'Neill, H. S. C.; Annersten, H.; Virgo, D. *Am. Mineral.* **1992**, *77*, 725.
(36) Sickafus, K. E.; Wills, J. M.; Grimes, N. W. *J. Am. Ceram. Soc.* **1999**, *82*, 3279.
(37) Bowen, L. B. *Mossbauer Eff. Ref. Data J.* **1979**, *2*, 76.

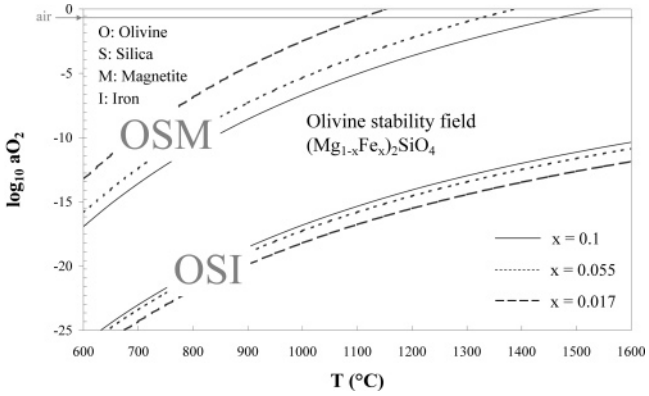

Figure 6. Temperature dependence of the thermodynamic stability of olivines $(Mg_{x-1}Fe_x)_2SiO_4$ determined on the basis of data from Nitsan.[38] Solid, dotted, and dashed lines represent the stability limits of olivines with $x = 0.10$, 0.055, and 0.017, respectively. OSI = equilibrium of olivine/silica/iron, OSM = equilibrium of olivine/silica/magnetite.

Table 5. Comparison of the Composition of Olivine (obtained by XRD and Mössbauer) as a Function of Calcination Temperature

	x (in $(Mg_{1-x}Fe_x)_2SiO_4$)		wt % Fe in the form of oxides	
T_{calc} (°C)	DRX	Mössbauer	DRX	Mössbauer
initial	0.048	0.055	3.7	3.1
1100	0.003	0.017	6.9	6.0
1400	0.025	0.020	5.3	5.7

the structure of olivine and 83% in the oxide form. However, calcination at 1400 °C does not lead to further iron extraction from the olivine structure, which confirms the XRD data. There is slightly more iron in the olivine lattice of the sample calcined at 1400 °C than in that calcined at 1100 °C. Table 5 compares the results of the olivine compositions determined by XRD and Mössbauer spectroscopy.

The values obtained by XRD and Mössbauer spectroscopy show a similar tendency. Calcination at 1100 °C permits us to extract approximately 6−7 wt % Fe. However, calcination at higher temperatures (1400 °C) gives a smaller quantity of iron in the form of oxides.

Thermodynamic Stability of Olivines $(Mg_{x-1}Fe_x)_2SiO_4$. The explanation for why the calcination of olivine at 1400 °C does not lead to further iron extraction from its structure lies in the thermodynamic stability of olivines. Figure 6 is based on Nitsan's thermodynamic data[38] and gives information on the thermodynamic stability of the olivine phase with different iron content levels.

The upper curves (OSM) represent the stability limits of olivines with different x values toward high-oxygen activities at which olivine, silica (SiO_2), and magnetite (Fe_3O_4 or $MgFe_2O_4$) coexist. The lower three curves (OSI) represent the stability limits of olivines with different x toward low-oxygen activities at which olivine, silica, and metallic iron coexist. The stability field of an olivine phase with a given iron content is between the OSM and OSI curves. Olivine of a given composition is thermodynamically metastable under O_2-T conditions falling outside the area enclosed by these curves.

Let us recall that the nominal olivine composition, taking into account the total iron content, corresponds to $x = 0.1$ (Table 1); according to the Mössbauer data, the initial olivine composition corresponds to $x = 0.055$ and this of olivine calcined at at 1100 °C to $x = 0.017$. The OSM and OSI curves for those values are indicated in the Figure 6. We can observe that the OSM curve shifts to lower temperatures with decreasing x; olivines with smaller x values become stable at lower temperatures because the oxygen activity corresponds to the composition of air.

A composition with $x = 0.017$ in air is stable at 1100 °C, and this composition is preserved after cooling to ambient temperature. Calcination at higher temperatures favors the stability of olivine with $x > 0.017$, confirming that further extraction of iron is not possible.

Conclusion for Olivine Oxidation. Taking into account the data from different techniques, we can conclude that the natural olivine used in this study initially contains a $(Mg_{0.94}Fe_{0.06})_2SiO_4$ phase with Fe^{2+} ions, small quantities of $MgSiO_3$, and iron oxides (~3 wt % iron) $MgFe_2O_4$ and probably α-Fe_2O_3. Calcination of the olivine leads to further oxidation.

The mechanism of olivine oxidation may be briefly summarized as follows

$$(Mg,Fe)_2SiO_4 \xrightarrow{400-1100\ ^\circ C} \underset{\text{forsterite}}{Mg_2SiO_4} + \underset{\substack{\text{amorphous}\\\text{silica}}}{SiO_2} +$$

$$\underset{\text{hematite}}{\alpha\text{-}Fe_2O_3} + \underset{\text{magnesioferrite}}{MgFe_2O_4} \xrightarrow{1100-1400\ ^\circ C} Mg_2SiO_4 + \underset{\text{enstatite}}{MgSiO_3} +$$

$$\underset{\substack{\text{hematite}\\\text{(traces)}}}{\alpha\text{-}Fe_2O_3} + \underset{\text{magnesioferrite}}{MgFe_2O_4}$$

During the calcination between 400 and 1100 °C, a large part of the iron is oxidized, as shown by Mössbauer spectroscopy. Calcination in the temperature range between 1100 and 1400 °C leads to the formation of the $MgSiO_3$ phase by reaction between olivine and silica. However, no more iron is extracted from the olivine structure; Fe^{2+} becomes more stable at higher temperatures, causing a small part of iron to be reintegrated into the olivine framework. The iron oxides α-Fe_2O_3 and $MgFe_2O_4$ are always present as secondary phases; however, their relative quantity depends on the temperature of calcination. It seems that α-Fe_2O_3 mostly forms at temperatures below 1100 °C, and the contribution of $MgFe_2O_4$ becomes more important after calcination between 1100 and 1400 °C.

Influence of the Calcination Temperature on the Reducibility of Natural Olivine. *Temperature-Programmed Reduction.* TPR was performed on olivine without pretreatment and on olivine calcined between 400 and 1400 °C (Figure 7).

Reduction profiles of the olivines calcined at different temperatures are similar, and only one reduction zone, with a maximum between 650 and 710 °C, depending on the calcination temperature, can be seen. This broad peak is attributed to the reduction of the free iron oxides (α-Fe_2O_3 and $MgFe_2O_4$) associated with the olivine structure. The intensity and width of the reduction peak increase with the temperature of calcination. Table 6 shows the percentage of reduced iron for olivine calcined at different temperatures, calculated from hydrogen consumption during TPR experiments.

(38) Nitzan, U. *J. Geophys. Res.* **1974**, *79*, 706.

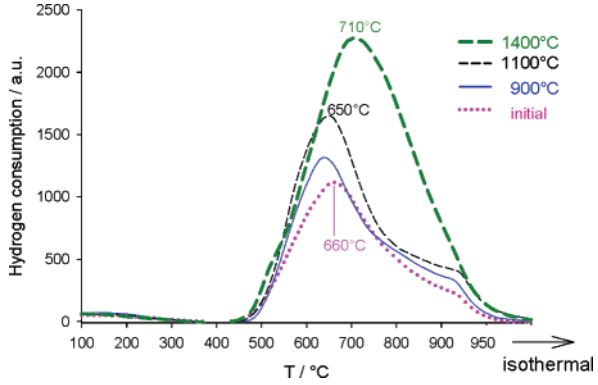

Figure 7. TPR of olivine calcined at different temperatures.

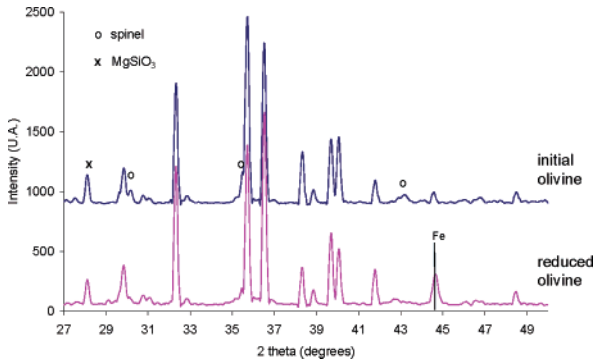

Figure 8. Diffractograms of natural olivine before and after reduction (λ = 1.5406 Å).

Table 6. Wt % Metallic Iron Obtained after the Reduction of Olivine Calcined at Different Temperatures

	wt % Fe	
T_{calc} (°C)	$Fe_{reduced}$/olivine	$Fe_{reduced}/Fe_{total}$
initial	1.4	20
900	1.6	23
1100	2.0	28
1400	3.2	45

The amount of reduced iron increases with calcination temperature. This could indicate that the free iron oxide content increases with the calcination temperature, what is not the case, as observed with XRD and Mössbauer spectroscopy. To explain this apparent controversy, we characterized the reduced olivine samples by XRD and Mössbauer spectroscopy.

Characterization of the Phases Observed after Total Reduction. *XRD.* Diffractograms of natural olivine after reduction (Figure 8) show that the main olivine phase is unchanged. On the other hand, the intensity spinel reflections decrease, and a new line appears at $2\theta = 44.6°$, which can be attributed to the main reflection of the metallic iron.[39] XRD patterns of olivine calcined at different temperatures and then reduced are similar.

Mössbauer Spectroscopy. To find the percentage of reduced iron in comparison to the quantity of free iron oxide, we applied Mössbauer spectroscopy for the reduced olivine samples.

Figure 9 presents the Mössbauer spectra of olivine calcined at 1100 and 1400 °C and then reduced by TPR.

(39) Powder Diffraction File 6-696 (Fe); International Center for Diffraction Data: Newtown Square, PA.

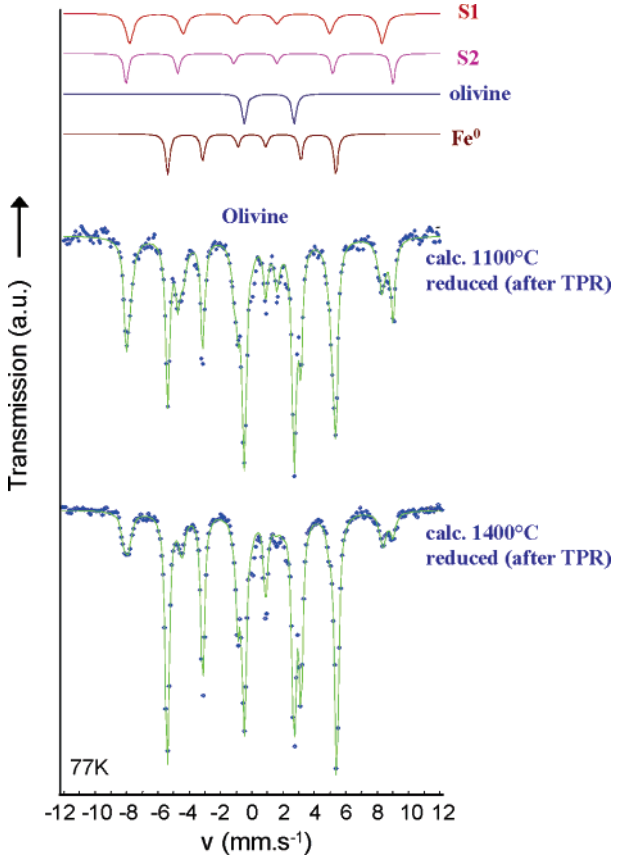

Figure 9. ^{57}Fe Mössbauer spectra at 77 K of olivine calcined at 1100 and 1400 °C after TPR; subspectra of the four components are indicated at the top.

Table 7. Mössbauer Parameters of Components Present in Olivine Calcined at 1100 and 1400 °C after TPR[a]

	olivine calcined at 1100 °C	olivine calcined at 1400 °C
	Doublet Fe^{2+} (olivine)	
δ (mm s^{-1})	1.18	1.18
Δ (mm s^{-1})	3.09	3.06
H (kG)	0	0
R (%)	26	27
	Sextet 1 Fe^{3+}	
δ (mm s^{-1})	0.26	0.23
Δ (mm s^{-1})	−0.03	0.02
H (kG)	497	497
R (%)	21	12
	Sextet 2 Fe^{3+}	
δ (mm s^{-1})	0.36	0.36
Δ (mm s^{-1})	0.28	−0.14
H (kG)	526	526
R (%)	18	7
	Sextet Fe^0	
δ (mm s^{-1})	0	0
Δ (mm s^{-1})	0	0
H (kG)	331	330
R (%)	35	54

[a] δ: isomer shift related to metallic iron; Δ: quadrupole splitting; H: hyperfine field; R: relative area.

The experimental spectra of reduced samples are a sum of four components: Fe^{3+} (S1 and S2), Fe^0, and Fe^{2+} (olivine). Table 7 gives the parameters that are characteristic of all components present in the reduced olivine samples.

All three components present in the olivine samples before reduction are still present in the reduced samples. The parameters of the third sextet (isomer shift equal to 0 mm

s^{-1} and hyperfine field of 330 kG) are characteristic of the metallic iron. The quantity of metallic iron is more important for the sample calcined at 1400 °C (54%) than for that calcined at 1100 °C (35%).

Table 8 shows a comparison of the iron distribution between different phases before and after reduction for olivine calcined at 1100 and 1400 °C.

We can conclude that Fe^{3+} from iron oxides is partially reduced (44 and 61%, respectively, after calcination at 1100 and 1400 °C), mostly to metallic iron and to a small extent to Fe^{2+}, which is reintegrated into the olivine structure (approximately 7−9%). The amount of metallic iron increases from 35% for the olivine calcined at 1100 °C to 54% for the olivine calcined at 1400 °C. This increase in the quantity of reduced iron is not related to the larger quantity of iron oxide. In fact, for the sample calcined at 1400 °C, the relative percentage of iron oxide is lower than that for the sample calcined at 1100 °C, as part of the iron is reintegrated into the olivine structure by calcination at 1400 °C.

The reason not all iron oxides are reduced and why they become more reducible after calcination at 1400 °C is the partial encapsulation of iron oxide particles by amorphous silica, as shown by McKernan and Carter,[40] who found by TEM the presence of a thin, continuous, amorphous silica film surrounding hematite islands in olivine annealed at 900 °C. We can consider that the protecting film of SiO_2 is also present at 1100 °C. At higher temperatures (1400 °C), amorphous silica reacts with olivine to form $MgSiO_3$,[24,25] facilitating the access of the reducing agent; more Fe^{3+} can be reduced, although its total amount decreases, as observed by Mössbauer spectroscopy.

Table 9 shows the comparison of the results of TPR and Mössbauer with respect to the quantity of metallic iron present in reduced samples.

Those values are comparable, taking into account the experimental incertitude.

In summary, the following schema can be proposed for the reduction of iron oxides produced during olivine's oxidation

$$\underset{\text{hematite}}{\alpha\text{-}Fe_2O_3} + \underset{\text{magnesioferrite}}{MgFe_2O_4} \xrightarrow{\text{reduction 950 °C}}$$

$$Fe^0 + Fe^{2+} + MgO \xrightarrow{Mg_2SiO_4} Fe^0 + (Mg,Fe)_2SiO_4 + MgO$$

Conclusions

The studied olivine with a nominal formula of $(Mg_{0.9}Fe_{0.1})_2SiO_4$ containing ∼7 wt % iron in its structure can be considered as being the most representative for the olivines that occur in nature. This olivine was initially calcined at 1600 °C to improve its mechanical resistance for fluidized bed use. The resulting initial olivine for our studies is in fact a system containing a $(Mg_{0.94}Fe_{0.06})_2SiO_4$ main phase, small quantities of $MgSiO_3$, and iron oxides (∼3 wt % iron) $MgFe_2O_4$ and α-Fe_2O_3. Calcination of this olivine in air leads to the oxidation of a part of Fe^{2+} from its structure with the formation of iron oxides (α-Fe_2O_3 and spinel-phase $MgFe_2O_4$) and other minority phases, such as amorphous SiO_2 (400−1100 °C) and $MgSiO_3$ (1100−1400 °C). The quantity of iron oxides formed by the oxidation of olivine depended on the calcination temperature. The maximum amount of free iron (∼6 wt %), in the form of Fe(III) oxides, can be obtained by calcination at 1100 °C and is limited by the thermodynamic stability of olivine.

Table 8. Distribution of Iron in Different Phases Obtained from Mössbauer Spectroscopy for Olivine Calcined at 1100 and 1400 °C before and after TPR

Type of Iron	*calc. 1100 °C*		*calc.1100 °C after TPR*	*% Fe^{3+} reduced*
Fe^{3+} (S1)	*29*	} *83*	*21*	*8*
Fe^{3+} (S2)	*54*		*18*	*36*
Fe^{2+} (olivine)	*17*		*26*	*Total = 44*
α-Fe^0			*35*	
Type of Iron	*calc. 1400 °C*		*calc.1400 °C after TPR*	*% Fe^{3+} reduced*
Fe^{3+} (S1)	*41*	} *80*	*12*	*29*
Fe^{3+} (S2)	*39*		*7*	*32*
Fe^{2+} (olivine)	*20*		*27*	*Total = 61*
α-Fe^0			*54*	

Table 9. Comparison of Quantities of Reduced Iron Determined by TPR and Mössbauer

	wt % Fe^0/olivine		$Fe_{reduced}/Fe_{total}$ (%)	
T_{calc} (°C)	TPR	Mössbauer	TPR	Mössbauer
1100	2.0	2.4	28	35
1400	3.2	3.8	45	54

Under reducing conditions, as shown by TPR and Mössbauer spectroscopy, only a part of the iron(III) oxides can be reduced to metallic iron (35 and 54% for olivine calcined at 1100 and 1400 °C, respectively). A small part (7−9%) of Fe^{3+} is reduced to Fe^{2+}, which reintegrates with the olivine structure. The remaining part of Fe^{3+} is probably the least accessible for the reducing agent because of an amorphous silica film surrounding the iron oxide particles. The quantity of metallic iron obtained after reduction varies from 1.4 wt % for the initial olivine to 3 wt % for olivine calcined at 1400 °C.

This study has shown the potential of an iron-bearing olivine, thermally treated in oxidating−reducing conditions, to produce metallic iron, which as previously proposed has an important role in the steam gasification of biomass. The calcination of olivine to extract iron oxides prior to its use in biomass gasification seems to be a very effective method for enhancing its activity.

To obtain an olivine with a high level of activity for tar elimination, it is desirable to extract the maximum amount of reducible iron from its structure. We have shown here the factors influencing both iron extraction from olivine and the reducibility of the resulting iron oxides using as the initial material an olivine calcined at 1600 °C. Keeping in mind the thermodynamic stability of olivines and the results presented here, we should find optimized conditions for a raw, noncalcined olivine. The key factors are calcination temperature and time, cooling rate, and reduction conditions

(40) McKernan, S.; Carter, C. B. *Ultramicroscopy* **1989**, *30*, 256.

for maximally extracting and reducing iron from its structure at minimal process costs. However, considering the use of olivine in a fluidized bed, we should also take the mechanical resistance of the final material into consideration; a double calcination, first to improve its mechanical resistance and then to extract more iron, can be of interest.

Acknowledgment. This work was carried out under EC-Project NNE5-2000-00212 (Contract ENK5-CT2000-00314). We thank the European Commission for its financial support. We also express our gratitude to Prof. J. Guille for carrying out the scanning electron microscopy observations.

CM051433+